



OAK RIDGE NATIONAL LABORATORY LIBRARIES



3 4456 0539373 0

ORNL/SUB-33200/2

Cy. 24

FUSION ENERGY DIVISION LIBRARY

JUN 20 '80

DEVELOPMENT PROGRAM FOR A 200 kW, CW GYROTRON

K. W. Arnold, J. J. Tancredi, M. Caplan, K. W. Ha,
D. N. Birnbaum, W. Weiss

QUARTERLY REPORT NO. 2 OCTOBER THROUGH DECEMBER 1979

Contract No. W-7405-ENG-26

FUSION ENERGY DIVISION LIBRARY

Prepared by

HUGHES AIRCRAFT COMPANY
Electron Dynamics Division
3100 West Lomita Boulevard
Torrance, California 90509

for
OAK RIDGE NATIONAL LABORATORY
Oak Ridge, Tennessee 37830
operated by
UNION CARBIDE CORPORATION
for the
DEPARTMENT OF ENERGY



ORNL/SUB-33200/2

DEVELOPMENT PROGRAM FOR A 200 kW, CW GYROTRON

**K. W. Arnold, J. J. Tancredi, M. Caplan, K. W. Ha,
D. N. Birnbaum, W. Weiss**

QUARTERLY REPORT NO. 2 OCTOBER THROUGH DECEMBER 1979

Contract No. W-7405-ENG-26

Prepared by

**HUGHES AIRCRAFT COMPANY
Electron Dynamics Division
3100 West Lomita Boulevard
Torrance, California 90509**

**for
OAK RIDGE NATIONAL LABORATORY
Oak Ridge, Tennessee 37830
operated by
UNION CARBIDE CORPORATION
for the
DEPARTMENT OF ENERGY**

TABLE OF CONTENTS

| <u>Section</u> | | <u>Page</u> |
|-----------------|---|-------------|
| I. | INTRODUCTION | 1-1 |
| II. | FREQUENCY REDIRECTION | 2-1 |
| | 2.1 General | 2-1 |
| | 2.2 Magnetron Injection Gun | 2-1 |
| | 2.3 Solenoid | 2-1 |
| | 2.4 RF Cavity | 2-2 |
| | 2.5 Power Supply | 2-2 |
| | 2.6 Test Equipment | 2-2 |
| | 2.7 Summary of Frequency Redirection Impact | 2-3 |
| III. | PROGRESS | 3-1 |
| | 3.1 General | 3-1 |
| | 3.2 RF Circuit | 3-1 |
| | 3.3 Electron Gun | 3-6 |
| | 3.4 Beam Analyzer | 3-7 |
| | 3.5 Power Supplies | 3-9 |
| | 3.6 RF Test Equipment | 3-9 |
| IV. | PROGRAM SCHEDULE | 4-1 |
| V. | BIBLIOGRAPHY | 5-1 |
| <u>Appendix</u> | | |
| A | DIAMAGNETIC LOOP FOR GYROTRON VELOCITY MEASUREMENTS | A-1 |

LIST OF ILLUSTRATIONS

| <u>Figure</u> | | <u>Page</u> |
|---------------|---|-------------|
| 1-1 | Schematic of gyrotron oscillator showing applied magnetic field and the rf field phase in the cavity. | 1-3 |
| 3.2-1 | TE ₀₂ mode in right cylindrical cavity. | 3-2 |
| 3.2-2 | TE ₀₂ mode in tapered cavity. | 3-4 |
| 3.2-3 | Efficiency vs. transit time (length) using an 8.5% magnetic field taper. | 3-5 |
| 3.4-1 | The induced flux produced by an electron beam moving at normalized velocity ($\beta = v/c$). | 3-8 |

I. INTRODUCTION

The objective of this program was the design and development of a millimeter-wave device to produce 200 kW of continuous-wave power at 110 GHz. The device, which will be a gyrotron oscillator, will be compatible with power delivery to an electron-cyclotron plasma. Smooth control of rf power output over a 17 dB range is required, and the device should be capable of operation into a severe time-varying rf load mismatch. During the middle of this report period, the operating frequency was changed to 60 GHz.

The technical baselines for the gyrotron and the associated power supply are shown in Table I. In the gyrotron, which is shown schematically in Figure 1-1, the electrons are formed into a hollow beam by a magnetron-injection electron gun with a considerable amount of their energy in rotation. A gradually rising magnetic field compresses the beam in diameter and at the same time increases the orbital energy according to the theory of adiabatic invariants until approximately 2/3 of the beam energy is in rotation and the rotational frequency is 60 GHz; at this point the magnetic field becomes uniform and the beam enters a quasi-optical open cavity where the spinning electrons interact with the eigen mode of the cavity. The rf energy builds up at the expense of the rotational energy of the dc beam. The spent beam enters the region of decreasing magnetic field, undergoes decompression and impinges on the collector. The latter also functions as the output waveguide. In order to handle the power in the spent beam and the power dissipation in the window the output waveguide tapers up from the cavity diameter to an appropriate value.

The duration of the program is 36 months, to encompass the building and test of up to twelve devices in addition to a beam analyzer and beam tester. The magnetron injection gun is well understood and allows

TABLE I

| <u>The Gyrotron</u> | |
|---|----------------------------|
| Frequency | 60 GHz |
| Power out | 200 kW RF |
| Electronic efficiency | 35% |
| Beam voltage | 70 kV |
| Beam current | 8.2 A |
| Magnetic field | 23.0 kG |
| Transverse to longitudinal velocity ratio | 1.5 |
| Cathode Loading | 4.5 A/cm ² |
| Cathode radius | 0.60 cm |
| Cathode length | 1.2 cm |
| <u>The Power Supply</u> | |
| Voltage rating | 100 kV dc |
| Current rating | 10 A |
| Anode supply voltage | 0-35 kV dc |
| Anode supply current | <200 mA |
| Heater supply voltage | 0-15 V, ac |
| Heater supply current | 15 A |
| Operating Modes: | |
| 1. | 10 μ s pulse length |
| 2. | 1 ms - 100 ms pulse length |
| 3. | 30 s to cw |

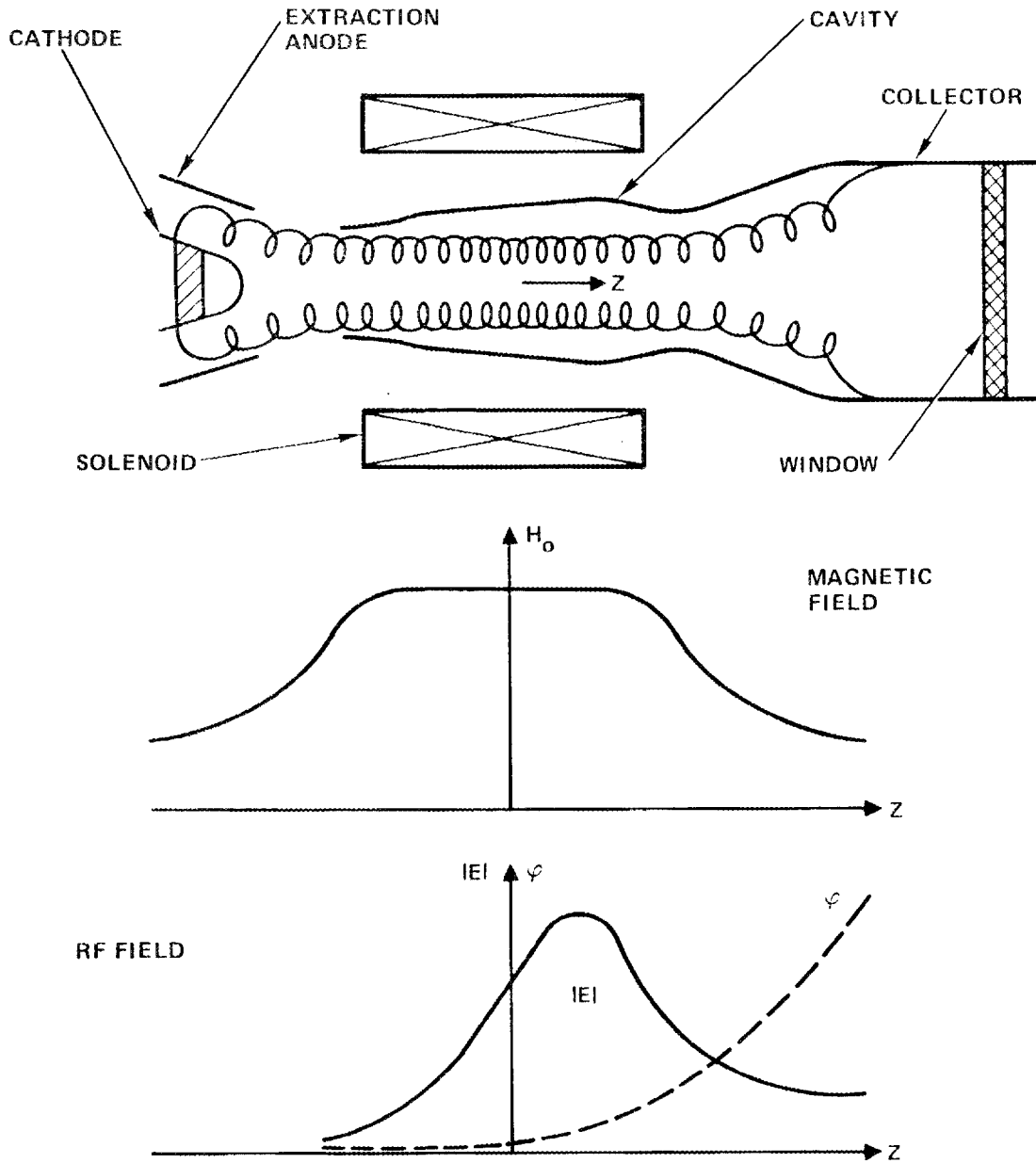


Figure 1-1 Schematic of gyrotron oscillator showing applied magnetic field and the rf field and phase in the cavity.

the use of the extraction anode (as well as cathode temperature variation) to vary the rf power out. At least two design approaches will be taken with respect to the collector, which has to be able to dissipate over 550 kW in undepressed operation. Fabrication and processing of prototype devices will proceed in parallel.

During this reporting period work was continued on a number of design tasks, including the magnetron injection gun, rf circuit, beam analyzer and power supply specifications. These activities are detailed in Section III of this report, following the delineation of relevant material pertinent to the frequency redirection.

II. FREQUENCY REDIRECTION

2.1 GENERAL

This development program began in June 1979 with an operating frequency of 110 GHz. On the basis of more current information, Oak Ridge has determined that the most urgent requirements for Electron Cyclotron Heating (ECH) are at a frequency of approximately 60 GHz. In response to this latter requirement, Oak Ridge has redirected this development program to 60 GHz. This frequency redirection has impacted the program schedule. The following paragraphs discuss the impact on specific tasks already underway.

2.2 MAGNETRON INJECTION GUN

The magnetron injection gun designed for the 110 GHz Gyrotron represents a compromise from optimum design values. The cathode current density of 8 Amps/cm² was higher than preferred, but was chosen because a reasonable velocity spread of 8 percent or less could be achieved. Lower current densities would have resulted in higher velocity spread. Consequently, a revised design approach is required for the 60 GHz gyrotron, which will lower cathode current density and velocity spread.

2.3 SOLENOID

The superconducting magnet designed for the 110 GHz produced a field of 1300 gauss over the cathode and 42.4 kilogauss in the cavity region. The axial separation between the cathode and cavity was approximately 23 cm. The 60 GHz design requires 23 kilogauss magnetic field in the cavity. Preliminary gun design for 60 GHz indicates that magnetic fields of 1300 gauss are required over the cathode. It therefore is plausible that a common superconducting magnet can be used for 60 and

110 GHz gyrotrons. The factor upon which this decision hinges is the required distance between the cathode and cavity for the 60 GHz gyrotron.

2.4 RF CAVITY

The proposed cavity design for the 110 GHz gyrotron would employ the TE_{02} mode, with the beam focused to the \vec{E} field closest to the axis. All of the cavity effort thus far has been applied to computer simulation and X-band cold tests. For the 60 GHz gyrotron, an identical approach will be employed, and since the effort to date has not been frequency selective, the cavity effort is applicable to both frequencies.

2.5 POWER SUPPLY

The power supply requirements for the 60 and 110 GHz requirements are very similar. Preliminary results on the magnetron injection gun reveal that the control anode voltage may be as high as 30 kV for the 60 GHz requirement, as opposed to 10 kV for 110 GHz. However, the power supply is to be capable of 35 kV modulation voltages. Therefore, no changes in the power supply specification are required.

2.6 TEST EQUIPMENT

No RF test equipment existed at Hughes for 110 GHz operation and therefore purchase orders were issued early in the program to overcome long lead times. At the time of the redirection in frequency, funds were irretrievably committed for 110 GHz equipment. RF test equipment at 60 GHz is either non-existent at Hughes or dedicated to other programs. Therefore additional equipment must be ordered for operation at 60 GHz. The lead time for this equipment is expected to be shorter than that for 110 GHz, and no impact on the schedule is anticipated at this time.

2.7 SUMMARY OF FREQUENCY REDIRECTION IMPACT

The major impact is in the area of gun design, and a possible redesign of the superconducting magnet. As a direct result of the additional design work required, the program schedule is expected to slip four months.

III. PROGRESS

3.1 GENERAL

Effort for this report period has been divided into the following tasks:

- RF Circuit
- Electron Gun
- Beam Analyzer
- Power Supply
- RF Test Equipment

3.2 RF CIRCUIT

The resonant frequency of cylindrical cavities can be readily calculated. The resonant frequencies of tapered cavities can be obtained with previously - reported computer codes¹. However, in determining the amount and location of the taper, it is important to understand how the cavity RF fields are affected. The existing Hughes computer code has recently been modified to provide better insight with respect to the E_{θ} fields within the cavity.

Figure 3.2-1a depicts a right cylindrical cavity, which is axially-symmetric about its axis (Radius=0). The contoured lines within the cavity represent \vec{H} field lines of a TE_{02} mode. The \vec{E} field is perpendicular to the plane of the paper, and peaks at two radial positions. The only component of \vec{E} for TE_{om} modes is E_{θ} .

Figure 3.2-1b illustrates how E_{θ} varies across the length of the cavity, peaked at the center of the axial distance and falling off uniformly at the ends of the cavity.

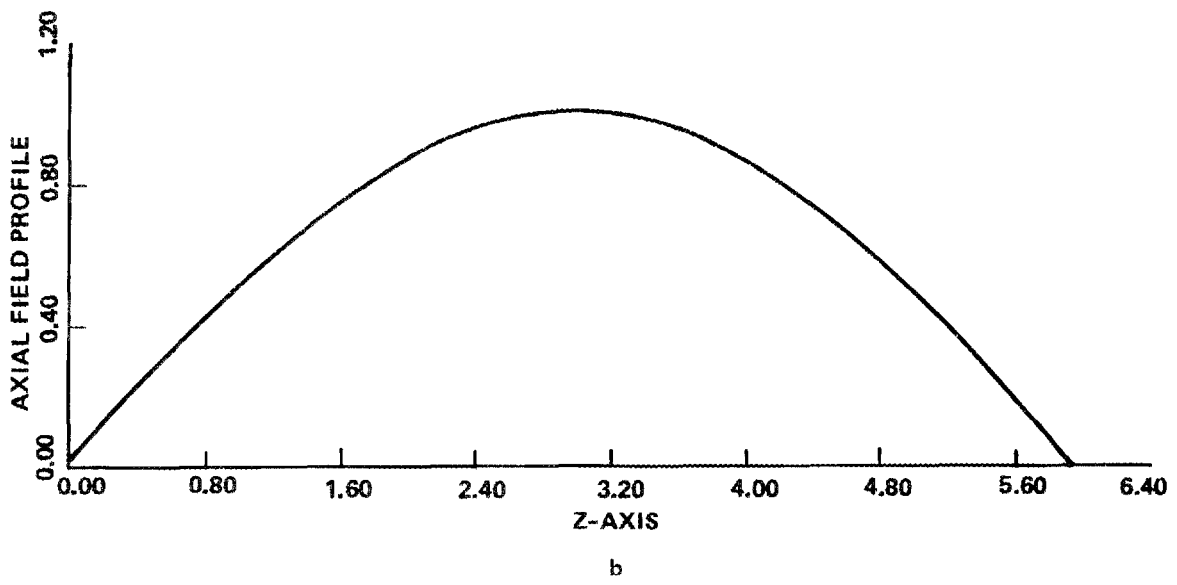
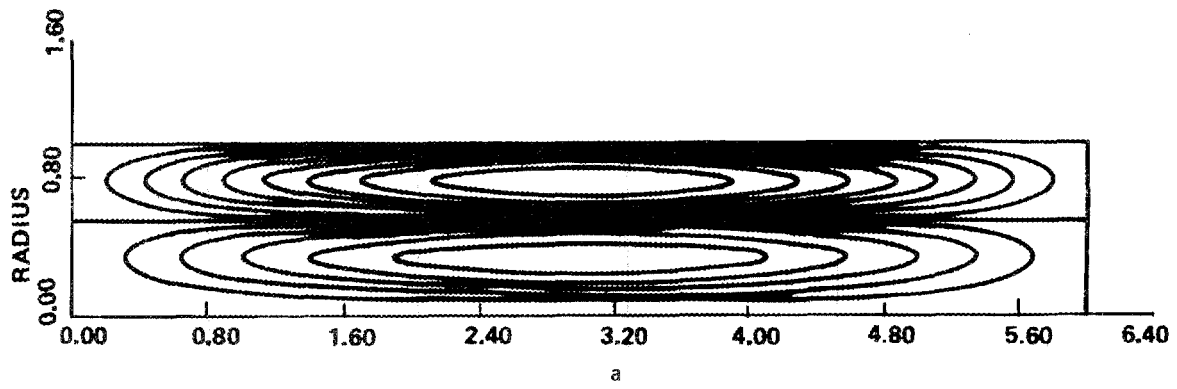


Figure 3.2-1 TE_{02} mode in right cylindrical cavity.

A tapered cavity is shown in Figure 3.2-2. The taper is only 5 percent of the normalized radius, yet the E_{θ} field peaks relatively sharply (Figure 3.2-2b) compared to Figure 3.2-1. Also noteworthy is the small peak at $Z=1.0$; this is a characteristic which appears many times in Soviet cavities.^{2,3} It is believed that this small peak serves as a prebuncher to enhance beam interaction.

Peaking of the E_{θ} field, on one hand, concentrates the interaction efficiently over a comparatively small region of the beam, but also concentrates the RF dissipation in the cavity walls over a small surface area. Thus, tapered cavities can create a heat dissipation problem, depending upon the actual heat lost into the cavity walls.

The heat lost to the cavity walls is dependent upon the Q of the cavity, and the Q is dependent upon the amount of power which leaves the cavity through the output iris. It is currently planned to modify the Hughes cavity computer code to evaluate various RF output conditions, and to determine the effect of these output shapes on cavity Q . At the same time, cold test cavities will be machined, at X-band frequencies, to enable measurement of Q using network analysis.

Recent interest in magnetic field tapering⁴ to enhance efficiency has prompted an analysis of a proposed 110 GHz gyrotron cavity and tapered magnetic field, utilizing the large signal computer program. The best results are shown in Figure 3.2-3. An efficiency of 56 percent could be attained by using an 8.5 percent magnetic field taper for the TE_{022} mode. The particular Q for this mode is 354. However, in order to be completely effective, the cavity had to be lengthened by almost 25%. Unfortunately, the Q for the TE_{022} mode is much lower than that for the TE_{021} , and would be difficult to excite.

This effort will continue through the next quarter.

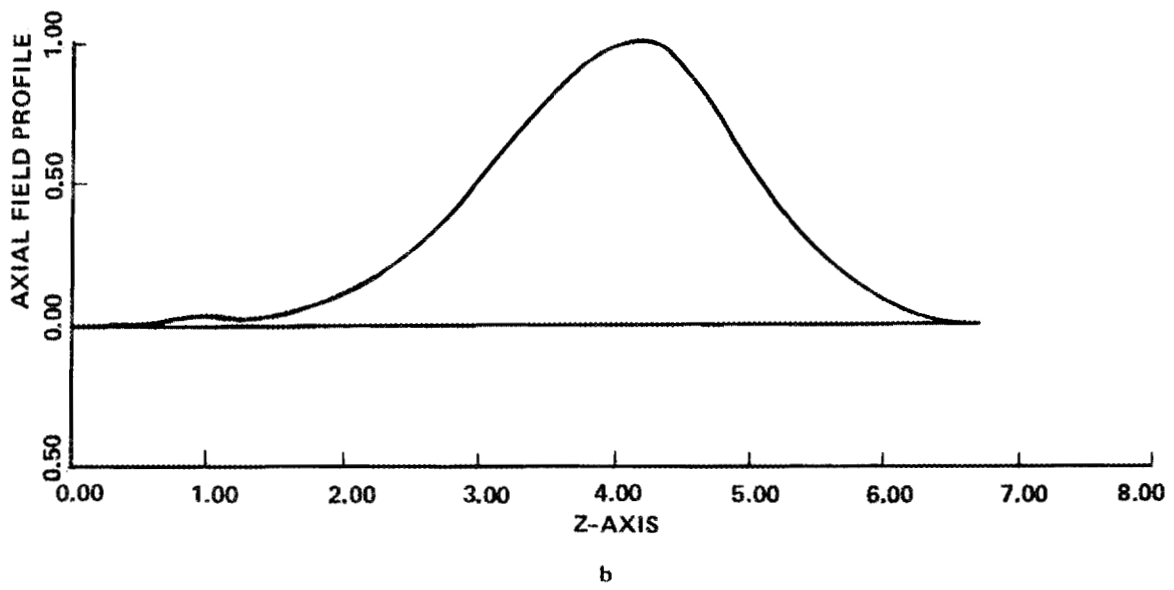
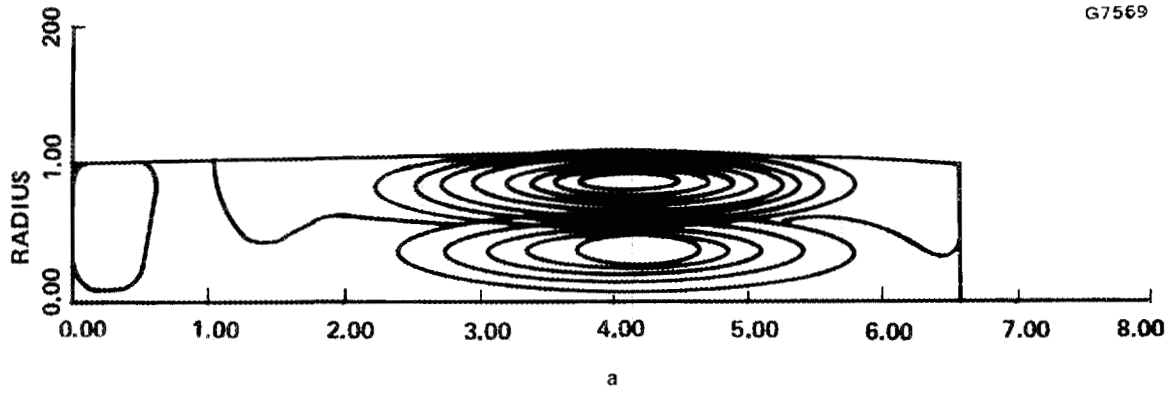


Figure 3.2-2 TE₀₂ mode in tapered cavity.

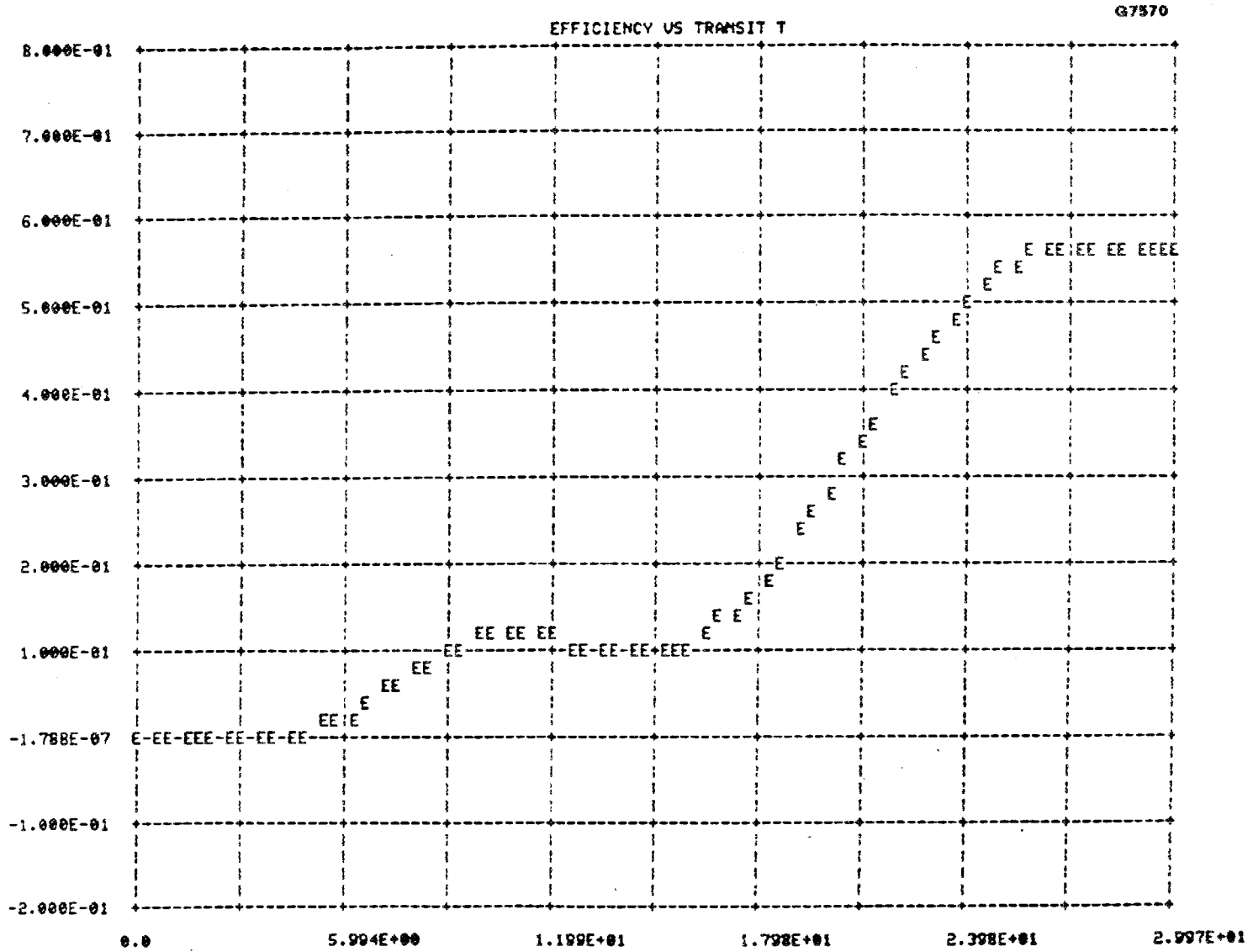


Figure 3.2-3 Efficiency vs. transit time (length) using an 8.5% magnetic field taper.

3.3 ELECTRON GUN

The magnetron injection gun is being redesigned for 60 GHz. Only a preliminary study has been completed to date. The results are shown in Table 3.3-1.

The salient features of the gun are that current density and ratio of temperature-limited current to space charge-limited current are reasonably low. Therefore, the feasibility of achieving a beam with low velocity spread is considerably better than for the 110 GHz gun. This latter gun achieved a v_{\perp} spread of less than 8 percent (based on computer trajectory calculations).

It is planned to continue effort on gun design until the design is optimized with respect to velocity, velocity spread, and magnetic field. Alternatively, it may be required to increase cathode current density to 5 or 6 A/cm² before the design can be fully optimized.

TABLE 3.3-1

| | |
|-------------------------|---------------------|
| Cathode Current Density | 4 A/cm ² |
| Cathode Radius (mean) | 0.6 cm |
| R_a/R_c | >2.0 |
| Cathode Angle | 15-25° |
| I_{TL}/I_{SC} | <10 percent |
| B_c | ≈1300 gauss |
| Anode Voltage | 22-29 kV |

3.4 BEAM ANALYZER

The purpose of the beam analyzer is to provide a means for verifying critical beam characteristics. One such characteristic is the amount of beam energy in rotation (proportional to v_{\perp}^2). Sophisticated techniques used in measuring beams for conventional microwave tubes, such as moving a "faraday cup" across the beam, are not readily applicable to beams where most of the energy is in rotation. Furthermore, measurements of the physical electron beam parameters are often costly to the program.

A plan has been put forth to perform gyrotron beam analysis by measuring the self-induced magnetic field produced by the beam. This induced field can be measured by means of non-energized, specially wound coils, called a diamagnetic loop. As the beam is pulsed on, an emf is produced in the special coils which can be measured on a scope. This emf measures the flux produced by the transverse beam energy. A complete derivation of the equations used is given in the Appendix.

The flux intercepted by n coils is:

$$\Phi \approx \frac{n I \gamma_o \beta^2}{B_o \beta_{||}} \quad (B_o \text{ in kilogauss})$$

Figure 3.4-1 illustrates the solution of this equation for n = 500 turns. At the design values of $\alpha (= \beta_{\perp} / \beta_{||}) = 1.5$, a flux of 128 maxwells will be intercepted by 500 turns.

As the beam is pulsed on, a flux change should be detectable on an oscilloscope, compared to the static flux of the solenoid. Calibration of the scope change can be accomplished by varying the known flux of the solenoid.

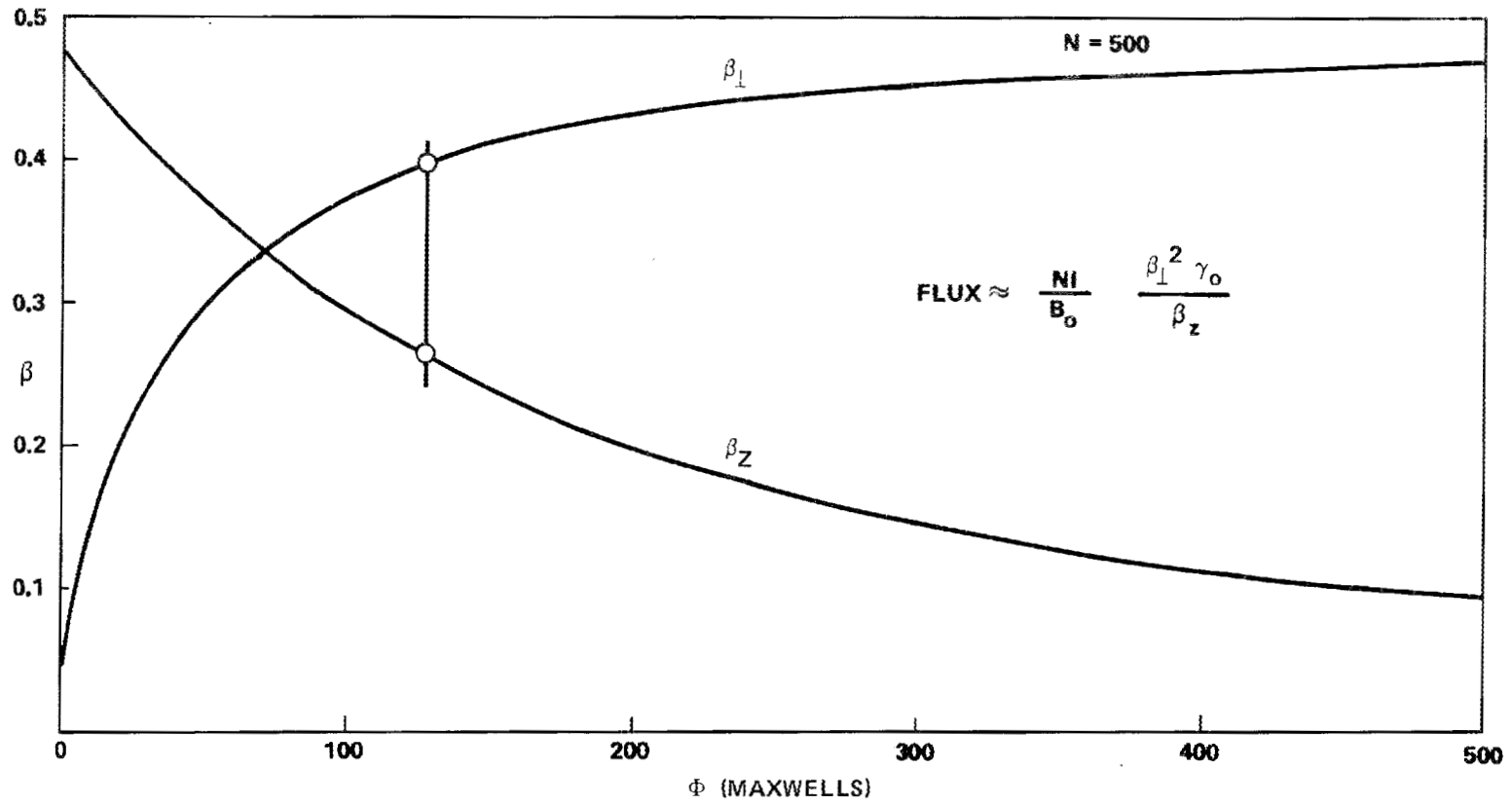


Figure 3.4-1 The induced flux produced by an electron beam moving at normalized velocity ($\beta = v/c$). The vertical line intersects β_{\perp} and β_z at $\alpha = 1.5$.

Implementing extra turns in the superconducting magnet does not appear difficult. Inactive coils are usually provided in these magnets to sense abrupt flux changes before the magnet goes "normal". The coils could be wound directly onto the outside of the warm bore tube, or over the gyrotron cavity itself.

3.5 POWER SUPPLIES

During the latter part of this report period, it was learned that equipment from the Missile Site Radar (MSR) on Kwajalein had become excess Army property. The radar transmitter contains a 150 kV high voltage supply with a capability up to 20 Amps DC. This power level is sufficient for a 1 MW gyrotron, which is an anticipated, long range DOE requirement. Because of this new development, the purchase of a new supply was postponed. Plans were made to view the existing equipment to determine its applicability for use at Hughes. These plans were to be implemented as soon as arrangements could be completed during the next report period.

3.6 RF TEST EQUIPMENT

The redirection to 60 GHz requires new cold test equipment. This equipment is expected to be ordered during the next report period.

Cold testing of various cavity designs will be conducted at X-band, initially. An Hewlett-Packard Network Analyzer has been made available on a part time basis for carrying-out this effort. Network analysis permits swept frequency measurements and displayed results on a Smith chart. Swept frequency measurements at 60 GHz do not appear to be feasible at this time.

The limited availability of circular waveguide components at the mm wave frequencies is cause for concern. Compounding the problem is the

high power level and TE_{02} mode at which development is required. The design and fabrication of circular waveguide components in-house appears necessary. Some design effort on circular-to-rectangular mode transducers has begun, based on work conducted by Hughes Culver City during the 1960's.

IV. PROGRAM SCHEDULE

4.1 PROGRAM SCHEDULE

A revised program schedule which reflects the frequency redirection is attached.

MILESTONE SCHEDULE AND STATUS REPORT — 60 GHz 200 KW GYROTRONS

| HUGHES EDD, TORRANCE, CA 90509 | | REPORTING PERIOD 12/79 | CONTRACT NO. FOR UNION CARBIDE CO., OAK RIDGE, TN. | | | | | | | | | | | | SHEET 1 OF 1 | | | | | | | | | | |
|--------------------------------|--------------------------------|------------------------|--|---|---|---|---|---------|---|---|---|---|---|---------|--------------|---|---|---|---|---|---|---|---|---|---|
| TASK NO. | TASK TITLE | FY 1979 | | | | | | FY 1980 | | | | | | FY 1981 | | | | | | | | | | | |
| | | J | J | A | S | O | N | D | J | F | M | A | M | J | J | A | S | O | N | D | J | F | M | A | M |
| 1100 | MAGNETRON INJECTION GUN DESIGN | A▽ | | | | | | B▽ | | | | | | C△ | | | | | | | | | | | |
| 1200 | DIODE GUN DESIGN | A▽ | | | | | | | | | | | | E▽ | | | | | | | | | | | |
| 1300 | SOLENOID DESIGN | | | | | | | A▽ B▽ | | | | | | | | | | | | | | | | | |
| 1400 | RF CIRCUIT DESIGN | A▽ | | | | | | B△ C△ | | | | | | | | | | | | | | | | | |
| 1510 | COLLECTOR 1. | | | | | | | A▽ B▽ | | | | | | | | | | | | | | | | | |
| 1520 | COUPLER 1. | | | | | | | A▽ B▽ | | | | | | | | | | | | | | | | | |
| 1610 | COLLECTOR 2. | | | | | | | | | | | | | A▽ B▽ | | | | | | | | | | | |
| 1620 | COUPLER 2. | | | | | | | | | | | | | A▽ B▽ | | | | | | | | | | | |
| 1900 | INTERFACE/LAYOUT | | | | | | | C▽ | | | | | | R▽ | | | | | | | | | | | |
| 2110 | BEAM | | | | | | | | | | | | | | | | | | | | | | | | |
| 2120 | BEAM ANALYZER FABRICATE | | | | | | | | | | | | | | | | | | | | | | | | |
| 2130 | BEAM ANALYZER TEST | | | | | | | | | | | | | | | | | | | | | | | | |
| 2210 | BEAM TESTER/ANALYZER DESIGN | | | | | | | A▽ | | | | | | | | | | | | | | | | | |
| 2220 | FABRICATE | | | | | | | | | | | | | A▽ | | | | | | | | | | | |
| 2230 | FOCUS TESTS | | | | | | | | | | | | | | | | | | | | | | | | |
| 2240 | THERMAL TESTS | | | | | | | | | | | | | | | | | | | | | | | | |
| 3110 | FABRICATE SN/1 | | | | | | | | | | | | | A▽ | | | | | | | | | | | |
| 3120 | TEST SN/1 | | | | | | | | | | | | | A▽ | | | | | | | | | | | |
| 3210 | FABRICATE SN/2 | | | | | | | | | | | | | | | | | | | | | | | | |
| 3220 | TEST SN/2 | | | | | | | | | | | | | A▽ | | | | | | | | | | | |
| 3310 | FABRICATE SN/3 | | | | | | | | | | | | | | | | | | | | | | | | |
| 3320 | TEST SN/3 | | | | | | | | | | | | | A▽ | | | | | | | | | | | |
| 5100 | POWER SUPPLY | A▽ | | | | | | E▽ | | | | | | C▽ | | | | | | | | | | | |
| 5200 | RF TEST EQUIPT | | | | | | | | | | | | | | | | | | | | | | | | |
| 6000 | REPORTS MONTHLY | ▽▽▽▽▽▽▽ | | | | | | | | | | | | | | | | | | | | | | | |
| | QUARTERLY | | | | | | | | | | | | | | | | | | | | | | | | |

4-2

V. BIBLIOGRAPHY

1. Arnold, K. et al., "Development Program for a 200 kW, CW, 110 GHz Gyrotron", Quarterly Report No. 1, June - September 1979, prepared by Hughes Aircraft Company for Oak Ridge National Laboratory under Contract W-7405-ENG-26.
2. Kurayev, A.A., F.G. Shevchenko, and V.P.S. Shestakovich, "Efficiency-Optimized Output Cavity Profiles that Provide a Higher Margin of Gyro-klystron Stability", Radio Engineering and Electronic Physics, vol 19, no. 65, pp 96-103, 1974.
3. Flyagin, V.A., et al, "Some Perspectives of the Use of Gyrotrons for Electron Cyclotron Plasma Heating in Large Tokamaks", paper presented at fourth International Conference on Infrared and Millimeter Waves, December 10-15, 1979, Miami Beach, Florida.
4. Read, M.E., et al, "Operating Characteristics of a 35 GHz Gyromonotron," Technical Digest of the International Electron Devices Meeting (IEEE), Washington D.C., December 3-5, 1979, pp 172-174.

APPENDIX A
DIAMAGNETIC LOOP
FOR GYROTRON
VELOCITY MEASUREMENTS

The use of diamagnetic loops for characterization of gyrotron beams is a concept extrapolated from a technique employed in plasma diagnostics¹.

A.1. MAGNETIC DIPOLE MOMENT

The magnetic dipole moment for the beam of Figure A-1, is defined as²:

$$\vec{m} = \frac{\pi I a_o^2}{c} \quad (\text{cgs units})$$

where

I = current due to a single electron

c = velocity of light

a_o = Larmor radius

The Larmor radius is further defined as

$$a_o = v_{\perp} / \omega_c$$

where

v_{\perp} = transverse electron velocity

and

ω_c = cyclotron frequency

$$\omega_c = \frac{e B_o}{\gamma m_o c}$$

G7572

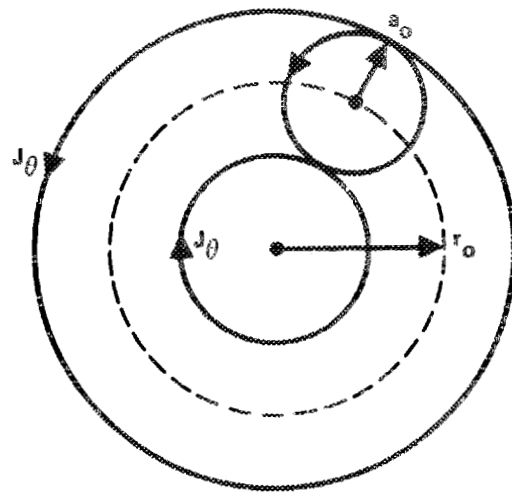


Figure A-1 Gyrotron beam cross-section.

where

- e/m_0 = charge-to-rest mass ratio
- γ = relativistic mass factor
- B_0 = steady state magnetic flux density

The electron current can be further defined as

$$I = \frac{e}{t}$$

where

t = time for one cyclotron orbit

$$t = \frac{2\pi a_0}{v_{\perp}} = \frac{2\pi}{\omega_c}$$

Therefore,

$$I = \frac{e \omega_c}{2\pi}$$

and

$$\vec{m} = \frac{\gamma m_0 v_{\perp}^2}{2B_0}$$

are the current and dipole moment due to a single electron.

A.2 MACROSCOPIC MAGNETIZATION

The magnetic moment per unit volume is often called the macroscopic magnetization. It is defined as

$$\vec{M} = N \cdot \vec{m}$$

where

N = is the number of electrons per unit volume.

A.3 EFFECTIVE CURRENT DENSITY

The magnetization contributes to the vector potential as an effective surface current density \vec{J}_θ :

$$\vec{J}_\theta = c(\hat{s} \times \vec{M})$$

where

\hat{s} is a unit normal vector to the surface

Therefore, on the outer surface, $\hat{s} \times \vec{M} = +\vec{J}_\theta$, and on the inner surface, $\hat{s} \times \vec{M} = -\vec{J}_\theta$, where:

$$J_\theta = c \cdot \vec{M} = c \cdot N \cdot \vec{m}$$

or

$$J_\theta = \frac{\gamma m_o c v_\perp^2 N}{2 B_o}$$

A.4 SELF-INDUCED MAGNETIC FLUX DENSITY

For steady-state magnetic fields,

$$\vec{\nabla} \times \vec{B}_i = \frac{4\pi}{c} \vec{J}$$

where

\vec{B}_i = induced flux density.

Taking the integral of the normal component of the above equation,
(see Figure A-2)

$$\int_S \vec{\nabla} \times \vec{B}_i \cdot \vec{n} \, dA = \frac{4\pi}{c} \int_S \vec{J} \cdot \vec{n} \, dA$$

where

S implies the surface shown in Figure A-2
 \vec{n} is in the direction normal to \vec{J} and \vec{B}_i

and

dA represents a differential area of S.

Applying Stoke's theorem for the line integral that lies inside the hollow beam,

$$\oint_C \vec{B}_i \cdot d\vec{\ell} = \frac{4\pi}{c} \int_S \vec{J} \cdot \vec{n} \, dA$$

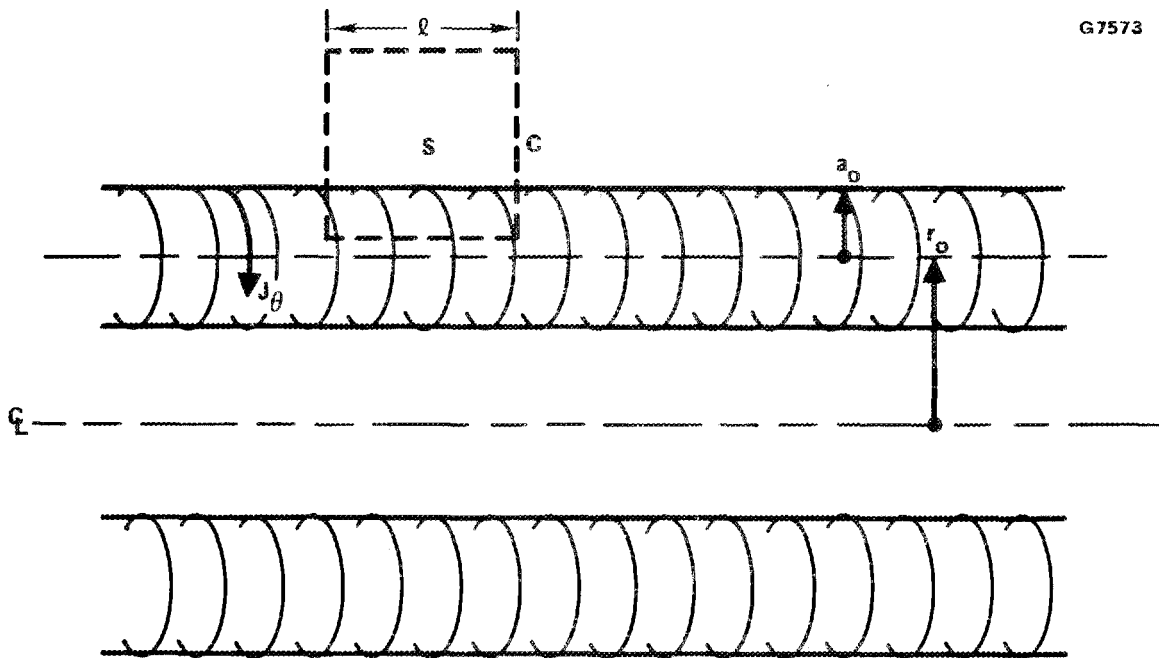


Figure A-2 Beam section showing plane for evaluating induced field.

which implies that the induced field in the z direction is:

$$B_i = \frac{4\pi}{c} J_\theta$$

Substituting for J_θ ,

$$B_i = \frac{2\pi\gamma m_o v_\perp^2 N}{B_o}$$

A.5 ELECTRON DENSITY

Let

$$\rho = \text{charge density} = Ne$$

Then

$$I = \rho \cdot \text{velocity} \cdot \text{cross-sectional area}$$

or

$$I = Ne v_\parallel 4\pi r_o^2 a_o$$

Solving for N,

$$N = \frac{I}{4\pi e v_{||} r_o a_o}$$

Substituting for a_o ,

$$N = \frac{I B_o}{4\pi v_{||} v_{\perp} \gamma m_o c r_o}$$

A.6 SOLUTION FOR INDUCED FLUX

$$B_i = \frac{2\pi \gamma m_o v_{\perp}^2}{B_o} \cdot \frac{I B_o}{4\pi v_{||} v_{\perp} \gamma m_o c r_o}$$

$$B_i = \frac{v_{\perp} I}{2 v_{||} c r_o}$$

Since in cgs units, I must be converted to Amps, the above equation can be rewritten:

$$B_i = \frac{v_{\perp} I}{20 v_{||} c r_o} \quad (I \text{ in Amps})$$

The flux from B_i which links n loops is:

$$\Phi = n B_i \cdot \text{Area}$$

Substituting:

$$\Phi = n \cdot \frac{v_{\perp} I}{20 v_{||} c r_o} \cdot 4\pi r_o a_o$$

or

$$\phi = \frac{n \pi I v_{\perp}^2}{5 v_{\parallel} \omega_c}$$

Substituting for ω_c , and using normalized velocities

$$\phi = \frac{n \pi I v_{\perp}^2 m \gamma_o c}{5 v_{\parallel} e B_o}$$

or

$$\phi = 1.07 \frac{nI}{B_o} \gamma_o \frac{\beta_{\perp}^2}{\beta_{\parallel}} \quad (\text{B in kilogauss})$$

This is the equation for induced flux, when the beam is turned on.

BIBLIOGRAPHY FOR APPENDIX

1. Carpenter, K.H. and Dandl, R.A., "Measurement of the Stored Energy in the Hot Electron Annuli of Elmo Bumpy Torus (EBT) by Means of Diamagnetic Pickup Loops," presented at the 21st Annual Meeting of the Division of Plasma Physics (APS), Session 6x2, Boston, MA 12-16 November 1979.
2. Jackson, J.D., CLASSICAL ELECTRODYNAMICS, John Wiley and Sons, Inc., N.Y., 1962, Chapter 5.

INTERNAL DISTRIBUTION

- | | |
|-----------------------|--|
| 1. L. A. Berry | 16. G. F. Pierce |
| 2. A. L. Boch | 17. T. L. White |
| 3. J. L. Burke | 18-19. Laboratory Records Department |
| 4. R. J. Colchin | 20. Laboratory Records, ORNL-RC |
| 5-8. H. O. Eason | 21. Y-12 Document Reference Section |
| 9. O. C. Eldridge | 22-23. Central Research Library |
| 10. R. P. Jernigan | 24. Fusion Energy Division Library |
| 11-13. C. M. Loring | 25. Fusion Energy Division Communications Center |
| 14. H. C. McCurdy | 26. ORNL Patent Office |
| 15. O. B. Morgan, Jr. | |

EXTERNAL DISTRIBUTION

27. R. A. Dandl, 1122 Calle De Los Serranos, San Marcos, CA 92069
28. A. N. Dellis, Culham Laboratory, Abingdon, Oxon, England, OX143DB
29. W. P. Ernst, Princeton University, Plasma Physics Laboratory, P.O. Box 451, Princeton, NJ 08540
30. W. Friz, AFAL/DHM, Wright Patterson AFB, OH 45433
31. T. Godlove, Particle Beam Program, Office of Inertial Fusion, Department of Energy, Mail Stop C-404, Washington, DC 20545
32. V. L. Granatstein, Naval Research Laboratory, Code 6740, Washington, DC 20375
33. G. M. Haas, Component Development Branch, Office of Fusion Energy (ETM), Department of Energy, Mail Stop G-234, Washington, DC 20545
34. J. L. Hirshfield, Department of Engineering and Applied Science, Mason Laboratory, 9 Hillhouse Avenue, Yale University, New Haven, CT 06520
35. H. Ikegami, Institute of Plasma Physics, Nagoya University, Nagoya 464, Japan
36. H. Jory, Varian Associates, 611 Hansen Way, Palo Alto, CA 94303
37. J. V. Lebacqz, Stanford Linear Accelerator Center, P.O. Box 4349, Stanford, CA 94305
38. K. G. Moses TRW Defense & Space Systems, 1 Space Park, Bldg. R-1, Redondo Beach, CA 90278
39. M. R. Murphy, Office of Fusion Energy (ETM), Department of Energy, Mail Stop G-234, Washington, DC 20545
40. V. B. Napper, Three Dunwoody Park, Suite 112, Atlanta, GA 30341
41. B. H. Quon, TRW Defense & Space Systems, 1 Space Park, Bldg. R-1, Redondo Beach, CA 90278
42. M. E. Read, Naval Research Laboratory, Code 6740, Washington, DC 20375
43. D. B. Rensen, General Atomic Company, P.O. Box 81608, San Diego, CA 92138
44. B. Stallard, Lawrence Livermore Laboratory, University of California, L-437, P.O. Box 808, Livermore, CA 94550
45. H. S. Staten, Office of Fusion Energy (ETM), Department of Energy, Mail Stop G-234, Washington, DC 20545
46. P. Tallerico, AT-1, Accelerator Technology Division, Los Alamos Scientific Laboratory, Mail Stop 817, P.O. Box 1663, Los Alamos, NM 87545
47. R. J. Temkin, National Magnet Laboratory, Massachusetts Institute of Technology, Cambridge, MA 02139
48. A. Trivelpiece, Science Applications, Inc., 1200 Prospect Street, P.O. Box 2351, LaJolla, CA 92038

EXTERNAL DISTRIBUTION (continued)

ORNL/SUB-33200C
2/15/80

49. Director, U. S. Army Ballistic Missile Defense Advance Technology Center, Attn.: D. Schenk,
ATC-R, P.O. Box 1500 Huntsville, AL 35807
- 50-51. Department of Energy Technical Information Center, Oak Ridge, TN 37830
52. RADC/OCTP, Griffiss AFB, NY 13441